ACS Catalysis

pubs.acs.org/acscatalysis

Research Article

Quantifying the Influence of Water on the Mobility of Aluminum Species and Their Effects on Alkane Cracking in Zeolites

Tram N. Pham, Vy Nguyen, Bin Wang, Jeffery L. White, and Steven Crossley*

Cite This: *ACS Catal.* 2021, 11, 6982–6994

Read Online

ACCESS | Metrics & More | Article Recommendations | Supporting Information

ABSTRACT: The role of extra-framework Al (EFAL) species on industrially important reactions such as alkane cracking has been extensively discussed and debated. It has long been known that water treatments influence the framework aluminum sites and, in some cases, can modify activity. What is less understood, however, is the direct relationship between the structural modifications and reactivity of important reactions such as alkane cracking and isomerization. The collective understanding of the multiple roles that water plays in the modification of zeolites and influence on reaction rates is continuously evolving. Extra-lattice Al species in close proximity to a framework Brønsted acid sites (BAS) have been proposed to modify the energies associated with surface intermediates and kinetically relevant transition states, which results in an enhancement in the rates of alkane cracking reactions. However, the kinetic role of water on the migration of these extra-framework alumina species to generate highly active sites is less understood and is the focus of this study. Water is introduced in controlled pulses to ZSM-5 zeolites with various Si/Al ratios and EFAL densities, with responses in *n*-hexane cracking activity used to investigate the generation of new active sites. A pulse technique allows decoupling of water dosing, lattice rearrangement, and drying, thereby enabling the quantification of activation energies associated with the generation of new active sites without losses in crystallinity or total BAS density. Further, by subtraction of the contributions to the reaction rate associated with isolated BAS, the reaction rate associated with the newly created sites is estimated. The results show that the energy barrier required for cracking on highly active sites is much lower than that observed on traditional Brønsted sites (75 vs 110 kJ/mol). The temperature dependence for the generation of these new sites reveals a 44 kJ/mol activation energy for the kinetically relevant step associated with their generation in the presence of water vapor, which to the best of our knowledge has not been previously quantified. It is reported that, while water vapor is essential for the generation of these new active sites, it also binds to these sites and strongly inhibits the cracking rate. These findings clarify some of the conflicting reports regarding the role of water in activity enhancement.

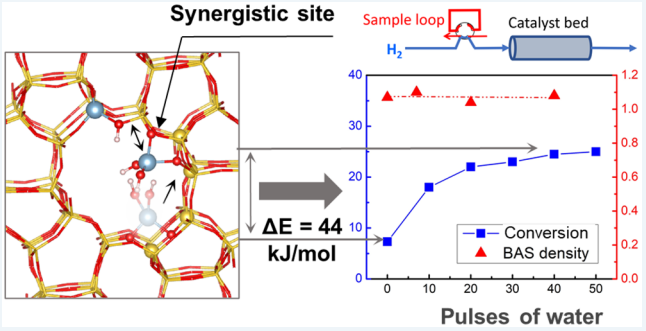

KEYWORDS: *HZSM-5, alkane cracking, extra-framework Al, steaming, rate enhancement*

1. INTRODUCTION

Zeolites are utilized widely as catalysts in many industrial reactions such as cracking, isomerization, and alkylation of different hydrocarbon molecules. Typical active centers are Brønsted acid sites (BAS) created by the charge balance of tetrahedrally coordinated aluminum atoms. The nature, number, and strength of these sites have been studied intensively for decades.[1,2] In addition to strong acidity, zeolites possess thermal robustness and flexibility in tailoring the shape, size, and connectivity of framework channels.

While it has been well established that modifying active sites by exposing zeolites to high-temperature steaming can lead to activity enhancement, consensuses regarding the mechanisms are difficult to attain. This is because the activity and selectivity within the microporous environments of zeolites are easily influenced by diffusion, and local confinement effects can play an important role in many reactions on zeolites.[3−6] Further, steam treatments often lead to modification of active sites in parallel with consequences on zeolite crystal structure such as the generation of mesopores and crystal collapse, all of which can affect catalytic activity.

It is well-known that the exposure of zeolites to moisture, even at room temperature, can lead to a variety of partially coordinated Al species in equilibrium with framework Al atoms. Some of these species have been suggested as being responsible for reactivity rates for facile low-temperature reactions such as H/D exchange. Our recent observations

Received: March 11, 2021
Revised: May 8, 2021
Published: June 1, 2021

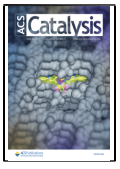

https://doi.org/10.1021/acscatal.1c01138
ACS Catal. 2021, 11, 6982–6994

that partially coordinated Al species can be removed by ammonium hexafluorosilicate (AHFS) washing and that there is some correlation between the concentration of these species and high-temperature cracking reactivity suggests that these could be precursors to form extra-lattice species under more severe conditions.[7,8] More severe steam treatments can lead to the removal of framework Brønsted acid sites to create extra-lattice species. Excessive exposure to high-temperature steam environments eventually leads to pore collapse; however, several studies report enhancements in catalytic activity after exposure to steam under mild conditions or for a short time for some reactions.[9−11] The extra-framework aluminum (EFAL) species created by dealumination during steaming could be responsible for these enhancements in catalytic activity in some instances. The migration of EFAL species upon steam treatment have been observed by quantitative 3D fluorescence imaging,[12] with resulting consequences on pore accessibility and furfuryl alcohol oligomerization activity. The nature of these EFAL species has been investigated, but the catalytic consequences of each are not completely known. Two general forms of EFAL have been proposed: cationic species including Al^{3+}, AlO^{+}, $Al(OH)^{2+}$, and $Al(OH)_2^{+}$ and polymerized or neutral compounds such as $AlO(OH)$, $Al(OH)_3$, and Al_2O_3. Several hypotheses have been proposed to explain the increase in activity observed for a variety of reactions over catalysts that contain extra-framework species, including higher acid strength,[13] enhanced heat adsorption of reaction intermediates,[14] and the polarization of alkane molecules by Lewis acidic sites.[15] Despite the variety of potential explanations, researchers generally agree that two types of Brønsted acid sites coexist, including isolated BAS (I-BAS) and synergistic sites, or acid sites where the activity is synergistically enhanced by the presence of extra-framework (EFAL) species near a traditional framework Brønsted site (EFAL-BAS). Many models have focused on the generation and rate enhancement on these synergistic sites.[7,11,14,16−19] Li et al. provided evidence for the detailed spatial proximities of Lewis/Brønsted acid sites in dealuminated HY zeolite by ^{1}H DQ-MAS NMR. They utilized NMR and density functional theory (DFT) calculations to reveal that EFAL species, such as $Al(OH)_3$ and $Al(OH)^{2+}$, could coordinate to the oxygen atom of the nearest BAS. The authors observed the downfield shift of the carbonyl carbon in ^{13}C NMR spectra of adsorbed 2-^{13}C-acetone as the hydrogen bond between the acidic proton and an oxygen atom of an adsorbent and attributed this to the increase in acidity of active sites.[17] An alternative explanation for enhancement of acidity by EFAL species has been proposed by Iglesia et al.[20−22] They claimed that the observed enhancement in activity is mainly associated with tighter confinement due to the presence of EFAL species, resulting in more stabilized transition states. Meanwhile, the acid strength determined by deprotonation energies is insensitive to the location and confinement of the corresponding framework Al atoms. NMR experiments combined with chemical washing with ammonium hexafluorosilicate (AHFS) were applied to study synergies between framework aluminum and EFAL species in these zeolites, revealing the emergence of a specific proton due to the presence of extra-lattice Al species that are removed after AHFS treatment.[7,23,24] Recently, Zhang et al. utilized pyridine and pentane adsorption while monitoring changes in the IR spectra to observe the interaction between EFAL oxide and acid sites. The authors claimed that the turnover frequencies of pentane cracking on these sites are about 52 ± 2 times higher than on isolated Brønsted acid sites.[18]

Part of the confusion surrounding alterations in zeolite structure and correlation to catalytic activity arise from the improper application of characterization techniques to study solid acids. For instance, ammonia is not considered as a good probe molecule to measure acid site strength by temperature-programmed desorption (TPD), as the peak temperature is strongly affected by diffusion and readsorption of ammonia within catalyst pores or along the catalyst bed. Reaction rates might be a more reliable indicator of the strength of a Brønsted acid site, but rates are also easily influenced by other factors such as diffusion, surface coverage, the confining environment surrounding an acid site, and the adsorption geometry.[5] Gounder et al. revealed that the estimation of framework aluminum content in faujasite zeolites by ^{27}Al MAS NMR spectra may not be accurate, as some distorted Al structures detected as framework Al sites are not associated with acidic protons, while other Al species may not be accurately quantified via NMR. This leads to disagreement in the number of protons measured by this technique in comparison with more reliable titration methods.[20] Conversely, relatively good agreement between ^{1}H solid-state NMR and IPA TPD has been achieved for the proton amount in some MFI catalysts.[7] In addition, depending on the identity of the coordinating species (such as H_2O, NH_3) and the temperature, coordinatively unsaturated aluminum species in these zeolites can reversibly convert between different forms: tetrahedral and octahedral coordination.[25,26] Therefore, the ^{27}Al MAS NMR representation at lower temperatures may not accurately reflect the concentration under the reaction conditions.

While much has been studied regarding potential stable species after steam treatments, one must note that the degree of enhancement in reaction rates is highly dependent on steaming conditions and initial zeolite Al distribution. The generation of synergistic sites is generally assumed to require an extra-lattice Al species in the proximity of a Brønsted site; however, this involves not only hydrolysis of framework Al to generate an extra-lattice site but also the subsequent migration of this extra-framework Al. The critical migration step has received much less attention than the initial hydrolysis. Further, it is well-known that, provided enough time in a high temperature steaming environment, these extra-lattice species may combine to form a more thermodynamically stable Al_2O_3 phase. It is highly challenging to decouple extra-lattice Al migration from its formation, limiting our ability to better understand the dynamic role of steam treatment on the generation of these synergistic sites.

It is generally accepted that selective monomolecular alkane cracking occurs at high reaction temperatures (≥450 °C), low reactant pressures, and low conversions, resulting in a simple product distribution. Many researchers utilize this reaction to investigate the catalytic activity or the acidity of zeolites.[9,11,14,15,27,28] The cracking of hexane, widely known as the α-test, has been used for decades as a probe reaction for a convenient measure of catalytic activity.[29,30] For instance, Haag et al. have reported that the activities per framework Al for hexane cracking are similar for a variety of as-synthesized HZSM-5 samples.[31,32] This activity is consistent with a variance of proton distribution and location within the catalysts studied. Therefore, in this work, we utilize hexane cracking to evaluate the activities of catalysts before and after water treatment. The role of water in the creation of synergistic

https://doi.org/10.1021/acscatal.1c01138
ACS Catal. 2021, 11, 6982−6994

sites is investigated over HZSM-5 zeolites of varying Si/Al ratios using a unique pulsed steaming approach. This method of water treatment is employed to inhibit the modification of the zeolite structure during continuous steaming and independently evaluate the role of water on Al migration independent of pore collapse and hydrolysis of framework Al species. Instead of exposing the catalyst to water vapor continuously, several pulses of water were introduced to change the activity of the catalyst for *n*-hexane cracking. After subsequent drying, this approach is demonstrated as an effective strategy to maintain the quantity of framework Brønsted sites while having a significant influence over cracking activity. Water pulses are compared with a continuous steam environment, and the resulting influence on the BAS density and activity of the catalysts is quantified. In addition, the results show that the BAS density and EFAL concentration in the parent material play an important role in the potential for activity enhancement by pulsing water treatments when additional dealumination is insignificant. Quantifying activity enhancements allow for measurement of activation energy associated with cracking over synergistic sites independently of isolated framework sites. Further, when these pulsed treatments are carried out as a function of temperature, the activation energy associated with the migration of EFAL species and creation of these sites themselves is measured, which is challenging or impossible to measure via other means.

2. EXPERIMENTAL SECTION

2.1. Catalyst Preparation. NH_4-ZSM5 catalysts with various Si/Al ratios were obtained from Zeolyst, and the HZSM22 catalyst was obtained from ACS Material. Catalysts were calcined at 873 K for 5 h in air with an initial slow ramp rate of 2 K/min to convert the NH_4^+ form to the H^+ form. Table 1 gives the catalysts used in this study and their physical properties. After calcination, all ZSM5 catalysts in proton form are indicated by HZSM5 followed by their Si/Al ratio. HZSM5-15 (Si/Al = 15) washed with ammonium hexafluorosilicate (AHFS), denoted as HZSM5-15-AHFS, was obtained using standard methods.[33] Additional details regarding the preparation and characterization of the HZSM5-15-AHFS sample utilized in this work have been described elsewhere.[7]

Table 1. Properties of Investigated Zeolite Samples

zeolite	Si/Al ratio	BAS density (mmol g^{-1}) calcd[a]	IPA-TPD[b]	lit.	calcd EFAL[c] (mmol g^{-1})
HZSM5-11.5	11.5	1.33	1.08	1.09[56,57]	0.25
HZSM5-15	15	1.04	0.73	0.76[7,16]	0.31
HZSM5-15-AHFS			0.70	0.74[7]	
HZSM5-25	25	0.64	0.48	0.54[16]	0.16
HZSM5-40	40	0.41	0.38	0.35[16,56]	0.03
HZSM-22	32.5–40	0.4–0.5	0.31		
HZSM5-140	140	0.12	0.10	0.094[57]	

[a]Calculated on the basis of Si/Al ratio and Al framework type. [b]Determined by IPA-TPD. [c]Determined by subtracting the theoretical BAS density by the number of BAS sites measured by IPA-TPD.

2.1.1. Water Pulsing/Steaming Zeolite. Several pulses of water with a partial pressure of 18.6 kPa were passed across the catalyst at 480 °C. The size of the loop and other conditions of pulsing water are described in section 2.3. Meanwhile, the steamed catalysts were obtained by exposing the catalysts to the same temperature and partial pressure of water vapor under an He flow (40 mL/min). It is noted that the water vapor pressures in these two cases are similar; however, the water vapor in the loop has a very short contact time (~0.1–0.2 s) with the catalyst bed carried by the He flow at 75 mL/min, while in steaming, catalysts were exposed to water all the time. A diagram of the pulse experiment is given in Figure S3.

2.2. Catalyst Characterization. *2.2.1. Surface Area and X-ray Diffraction Measurements.* N_2 physisorption was carried out at −198 °C on a Micromeritics ASAP 2010 instrument. The samples were degassed for 10 h under vacuum at 250 °C prior to the absorption. X-ray diffraction (XRD) studies of catalysts were conducted on a Rigaku diffractometer, utilizing Cu Kα radiation generated at 44 mA and 40 kV; the diffraction angle range was 2θ = 2–70°.

2.2.2. Solid-State NMR Spectroscopy. ^{1}H MAS NMR spectra were collected on a Bruker Avance 400 spectrometer. The details of the procedure and conditions of the measurement have been described elsewhere.[7,23,24]

2.2.3. IPA TPD Experiment. The density of BAS was measured by the temperature-programmed desorption of isopropylamine (IPA-TPD). The catalyst was pretreated at 480 °C, the temperature of the cracking reaction, for 2 h to remove moisture and cooled to 100 °C under a helium flow of 30 mL/min. Then, it was exposed to 2 μL pulses of IPA. After that, weakly adsorbed IPA was removed from the catalyst by flushing He for few hours at the same temperature. The catalyst was heated to 600 °C with a 10 °C/min linear heating ramp. A sharp peak of propylene as a product of the reaction between Brønsted sites and IPA was observed at the high-temperature range of 300–390 °C. This peak was used to determine the number of Brønsted sites. The analysis was elaborated by utilizing an MKS Cirrus mass spectrometer, tracking m/z 17, 41, and 58 for ammonia, propylene, and IPA, respectively. The intensity of the propylene signal (m/z 41) was calibrated by several 500 μL pulses of propylene.

2.3. Kinetic Measurements. The activity of each catalyst for the conversion of *n*-hexane cracking was evaluated by a micropulse reactor at 120 kPa pressure using helium as the carrier gas. A 5–70 mg amount of catalyst pelletized to 0.25–0.35 mm particles and then mixed with glass beads was used for the reaction. Before reaction, the catalyst was treated at the reaction temperature of 480 °C for 2 h with a 75 mL/min helium flow. Several pulses of the hydrocarbon reactant diluted in helium (0.48 μmol of HC/pulse, 3.7 mol % of HC in He) were then sent over the catalyst bed. The size of the loop was 500 μL. During the period between continuous pulses, the catalyst was exposed to a helium flow. A Shimadzu QP-2010 GCMS/FID system using a HP-PLOT/Al_2O_3/"S" column connected to the reactor outlet was applied to analyze the products of the reaction.

2.4. DFT Calculations. All DFT calculations were carried out using the Vienna *ab initio* simulation package (VASP).[34] The projected augmented wave (PAW)[35,36] method and the GGA-PBE exchange correlation function[37] were used. To include van der Waals interactions, the DFT-D3 semiempirical method[38] was employed. The HZSM-5 unit cell used in all calculations consists of 96 T sites and 192 O atoms. The lattice constants were set to a = 20.078 Å, b = 19.894 Å and c = 13.372 Å as in our previous studies.[7,8,39] The structure was fully relaxed until the atomic force was smaller than 0.02 eV

https://doi.org/10.1021/acscatal.1c01138
ACS Catal. 2021, 11, 6982–6994

$Å^{-1}$. The kinetic cutoff energy was set to 400 eV. To assess the migration of $[Al(OH)_2]^+$, the migration barriers were investigated at the intersection. A framework Al site was set at T10 in a five-membered ring to compensate the charge of the EFAl cation. At the intersection, $[Al(OH)_2]^+$ migrated from a position facing a T7 site to one facing a T11 site and then to one close to a T12 site. The nudged elastic band (NEB)[40] method was used to calculate the transition state.

3. RESULTS AND DISCUSSION

3.1. *n*-Hexane Cracking. The interpretation of reaction rates when feeds are pulsed across a catalyst is different from that of a continuous-flow reactor.[41,42] The partial pressure of *n*-hexane exhibits a Gaussian peak, as can be seen in Figure S1, with the overall conversion used to measure the average activity of the catalysts. To more precisely reflect the rates for kinetic measurement purposes, the rate is reported as an averaged rate over the entire pulse, while the partial pressure is varied by modifying the concentration of *n*-hexane in the loop. More details regarding the analysis of rate and activation energies in this reactor are provided in the Supporting Information. No significant deactivation is observed over the course of the experiment under the conditions used in this study. The order of the reaction at various temperatures on HZSM-5 catalysts is close to 1, as shown in Figure 1, which along with the product distribution, shown in Figure S1, suggests a monomolecular cracking mechanism in agreement with literature reports.[43] The alkane/alkene ratios deviate from unity due to secondary reactions such as cracking of hexenes and pentenes, enhancing the selectivity to lighter alkenes.

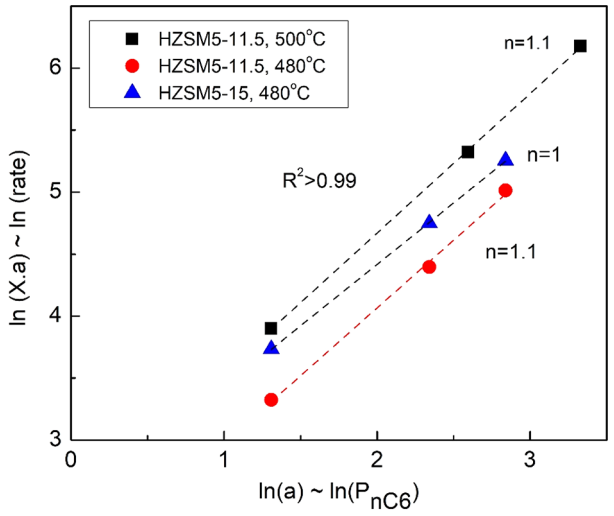

Figure 1. Determination of order of *n*-hexane cracking reaction, where *a* is the mole percent of *n*-hexane in the loop and *X* is the conversion of the reaction (see the Supporting Information).

3.2. Role of Acid Site Proximity and Extra-framework Aluminum. Figure 2 presents the catalytic activity per site of catalysts of various HZSM-5 catalysts. The discrepancy in turnover frequency values could be explained by the greater concentration of EFAL species, in the various catalysts. While prior reports have indicated that the rates of alkane cracking over isolated BAS (I-BAS) are much lower in comparison to those over synergistic sites (EFAL-BAS),[18] the activity observed is influenced by both. It is important to note that the conversion is reported after normalizing per mol_{BAS}; thus, activity enhancements beyond the value reported for the AHFS-washed HZSM5-15 (where the number represents the Si/Al ratio) catalyst reflects rate enhancements due to the presence of synergistic sites. HZSM5-140, HZSM5-40, and HZSM5-15-AHFS catalysts have insignificant amounts of EFAL in their structure. As a result, the activities per site are comparable for these catalysts. The activities per site of these catalysts should reflect the activity of isolated Brønsted sites. HZSM5-40 has a slightly higher activity per site since it has a very small population of synergistic sites. The activity of HZSM5-140 is lower than that of HZSM5-15-AHFS, which could be attributed to the difference in either BAS density or the distribution of acid sites in these two catalysts.[28,44] Note that, for all of the catalysts tested, those with a higher BAS density such as HZSM5-25, HZSM5-15, and HZSM5-11.5 also exhibit a greater fraction of Al species that are not framework BAS in their structure. This suggests that BAS proximity and/or the EFAL density might play an important role in the activity enhancement. The parent HZSM5-15 and the AHFS-washed HZSM5-15 catalysts for the selective removal of EFAL species have the same framework Al densities on the basis of IPA TPD; however, their catalytic activities are significantly different. This illustrates that acid site proximity or density alone cannot be responsible for the loss in activity of the AHFS-washed HZSM5-15, which must be related to the absence of EFAL species. If the EFAL species is in the vicinity of a framework BAS, a synergistic site having higher activity could be generated. It is logical to assume that catalysts with higher BAS density will have more framework sites in close proximity and therefore a local charge that encourages interaction of EFAL cationic species in the vicinity of an adjacent BAS. As a result, a higher initial site density (more

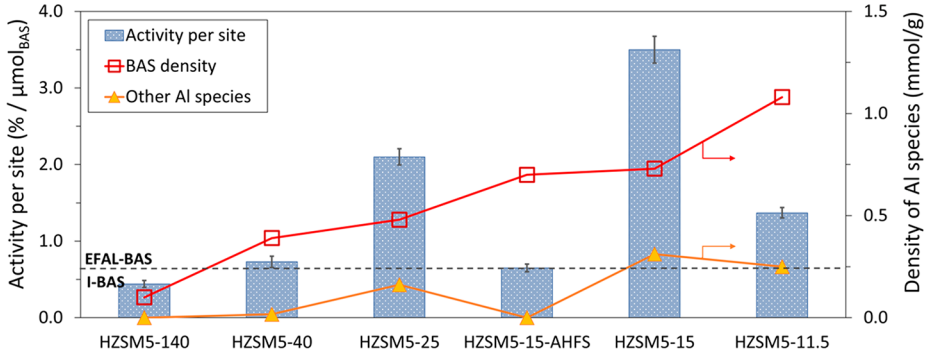

Figure 2. Conversion of *n*-hexane cracking per site on various HZSM5 catalysts. Reaction conditions: T = 480 °C, P_{nC6} = 4.5 kPa with 0.48 μmol of *n*-hexane injected in each pulse, amount of catalysts varied to achieve conversions within 5−15%.

https://doi.org/10.1021/acscatal.1c01138
ACS Catal. 2021, 11, 6982−6994

sites in close proximity) should exhibit a greater potential for the formation of synergistic sites, given the presence of EFAL cationic species. This hypothesis is evidenced by the higher activity enhancement due to water treatment of higher BAS density catalysts, discussed in section 3.3. As previously stated, the activity is affected by not only the BAS density but also the presence of EFAL. The fact that the activities of HZSM5-25 and HZSM5-15 are higher than that of HZSM5-11.5 could be explained by the higher fraction of EFAL over framework Al leading to a higher possibility to create more synergistic sites in the parent zeolites. We acknowledge that the generation of synergistic sites might be affected by not only the EFAL concentration but also the migration of EFAL species and the ability of the zeolite structure to stabilize them in an environment necessary to create the synergistic sites. For instance, DFT calculations from Silaghi et al. suggest that the thermodynamic stability of hydrated EFAL species depends highly on the local confining environment, with the channel intersections being the most preferred locations for EFAL cations.[45] Follow-up studies focusing on the form of EFAL species and other factors such as the number of paired sites and the location of the framework Al are needed in the future, as all of these may influence the formation of synergistic sites.

3.3. Water treatment by Steaming and Pulsing. *3.3.1. Difference between the Two Methods.* A clear distinction exists when a zeolite is subjected to a continuous partial pressure of steam vs very small water pulses. This is clear by observing the discrepancy in BAS evolution and resulting activity for *n*-hexane cracking when the two methods are applied. Figure 3 presents the change in the activity during these two treatments.

First, we discuss implications on the rate due to pulsing water. The catalysts were exposed to several pulses of 2.85 μmol of water spaced at 10 min intervals, followed by 3−10 h of drying under a He flow. The activities were measured by conducting the reaction with pulses of *n*-hexane. The drying time depends on the number of pulses of water that catalysts were exposed to during the water treatment. The activities of the catalysts were determined when at least two continuous pulses of hexane gave the same conversion. The BAS densities of the catalysts were measured via IPA TPD after different batches of catalysts were exposed to 10, 20, and 40 pulses of water. No measurable loss in BAS density is observed when HZSM5-11.5 is treated by sequential pulses of water, and the potential for BAS losses is expected to be even less significant for catalysts with a lower BAS density. In addition, no significant changes in the product distribution and the order of the reaction are observed as the catalytic activity is modified by water treatment. To compare product selectivities at isoconversion, a higher loading of HZSM-5 in the absence of water treatment was compared with the catalysts after exposure to water pulses, and the product distribution of the two cases are not significantly altered (see Figures S1 and S2 in the Supporting Information). These results suggest that the water treatment modifies the activity of the catalyst but not the reaction mechanism. Further, the lack of shift in selectivity while clearly the activity within each crystallite is enhanced indicates that these results are not influenced by internal diffusion within the zeolite crystals.

In contrast with the pulsing results, catalysts were also exposed to steaming conditions where a consistent stream of water vapor at the same partial pressure as that described in the pulse loop above was passed across the catalyst for prolonged

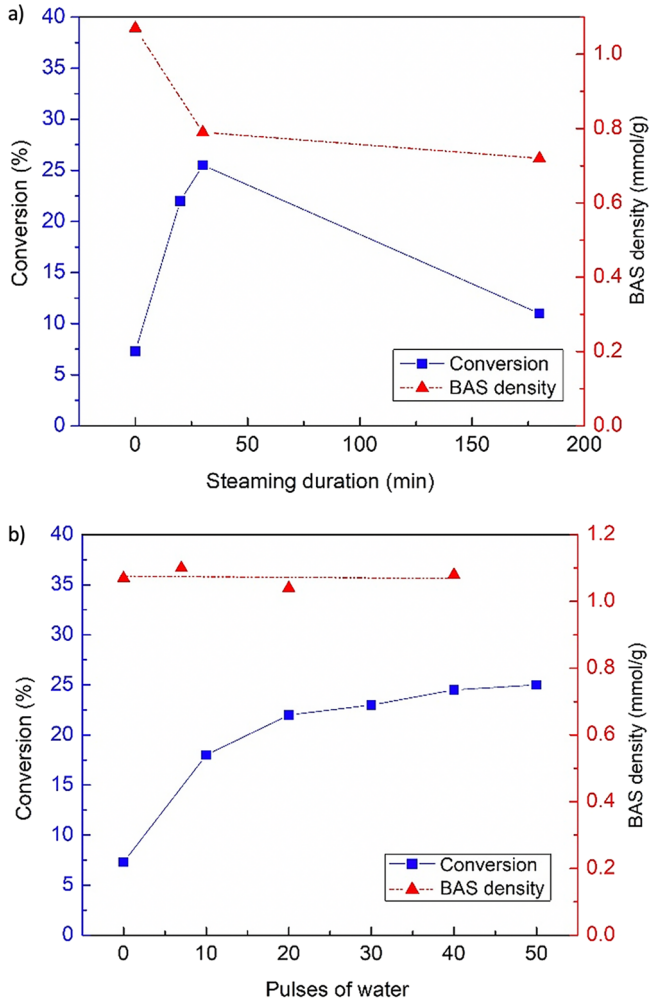

Figure 3. Conversion of *n*-hexane cracking on HZSM5-11.5 catalyst and BAS density (determined by IPA-TPD) as a function of (a) steaming duration (catalyst was treated by steaming) and (b) number of pulses of water (catalyst was treated by pulsing water). The steam treatment was at 480 °C in both cases, with a water partial pressure of 18.6 kPa either in a continuous manner or in pulses. Reaction conditions: T = 480 °C, P_{nC6} = 4.5 kPa with 0.48 μmol of *n*-hexane injected in each pulse, 5 mg amount of catalyst. The BAS densities of HZSM5-11.5-0.5hS and HZSM5-11.5-3hS are 0.79 and 0.73 mmol/g, respectively. A diagram of pulse experiment is given in Figure S3.

times. After steaming, the catalyst was dried overnight prior to performing the *n*-hexane activity tests. In contrast to the pulsing techniques, the more common continuous steaming exhibited an enhancement of catalytic activity followed by a decrease after prolonged steam exposure, in good agreement with prior observations by Lercher and co-workers.[18,46] Nitrogen absorption indicates that the surface areas of HZSM5-11.5 catalysts are comparable, ∼ 345−353 m^2/g, as shown in Table S1, which are comparable with values reported elsewhere.[7] In addition, the XRD patterns of these samples shown in Figure 4 indicate that the crystallinity of the zeolites was not significantly altered due to water treatments.

The results also show that the activity of the catalyst is increased approximately 3−3.5-fold by both methods of treatment. In the cases of pulsing water, the activity of the catalyst does not change after reaching the maximum, while in steaming, the activity passed through the maximum and decreases quickly with prolonged steaming times. Since it was

https://doi.org/10.1021/acscatal.1c01138
ACS Catal. 2021, 11, 6982−6994

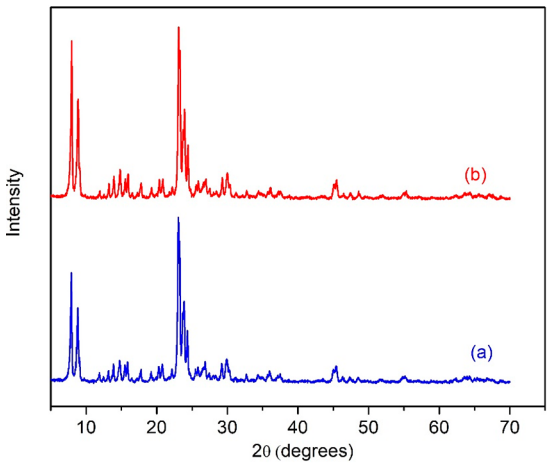

Figure 4. XRD patterns of (a) fresh HZSM5-11.5 and (b) HZSM5-11.5-3hS.

hypothesized that the activity is increased by the generation of synergistic sites, it is likely that, in the pulsing experiment, the catalytic activity will increase until the maximum number of proximate of Brønsted acid sites and active EFAL species in the structure is achieved. These synergistic sites are metastable species that remain for the duration of the pulse treatments. In contrast, when a continuous steam treatment is used, the number of Brønsted sites diminishes due to either dealumination or pore collapse. Further, extended steam treatments may eventually lead to the migration of these metastable synergistic sites to form Al_2O_3 clusters. The rate of these events depends on steaming time, water partial pressure, and temperature of the treatment. The IPA-TPD results show that, under the conditions of steaming treatment in this study, the Brønsted acid site density is rapidly reduced after short steaming times, about 25% loss after 30 min, with a diminished rate of decrease in BAS density with prolonged steaming times, in agreement with literature reports.[46]

Figure 5 illustrates ^{1}H MAS NMR spectra of the parent HZSM5-11.5 catalyst, the HZSM5-11.5 sample after exposure to 50 pulses of water, and two others with different steaming durations. The spectra show that there are no significant modifications of the catalyst treated by pulsing water in comparison to the parent zeolites; therefore, the activity enhancement must be related to the mobility of EFAL species. Since the loss of BAS represented by the peak at 4.2 ppm is compensated by the generation of AlOH species not classified as traditional framework BAS species, both steaming samples show increases in the peak corresponding to non-BAS AlOH species located at 2.8 and 12−15 ppm in comparison with the fresh catalysts. The signal at 2.8 ppm is commonly attributed to AlOH species,[47] with the corresponding 12−15 ppm peak attributed to framework/extra-framework interactions in both HZSM5[7] and HFER catalysts.[48] Recently, the appearance of these two signals in the ^{1}H NMR spectra of HZSM5 catalysts has also been attributed to Al−OH species that are best described as partially coordinated framework species.[8,24,49,50] However, these partially coordinated species can also be precursors to the generation of EFAl species after exposure to more severe conditions,[45] which may then interact synergistically with existing framework sites through a variety of previously proposed mechanisms.[17,51] For the purpose of this analysis, the presence of these features is solely meant to

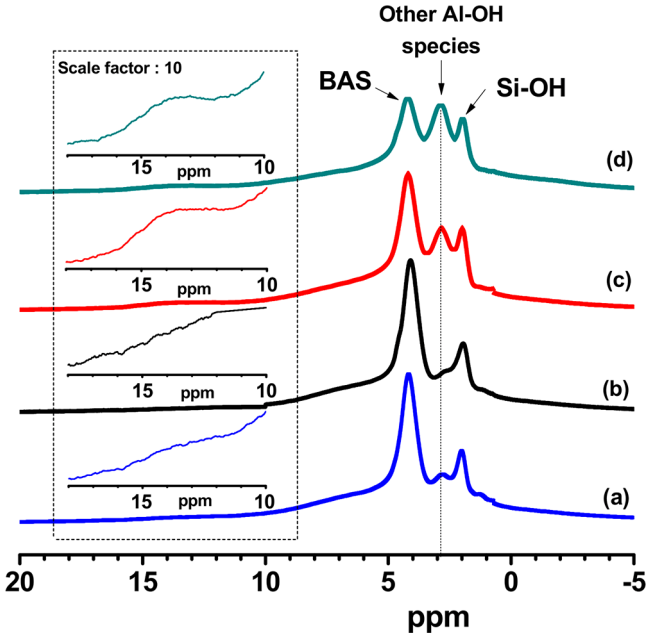

Figure 5. ^{1}H MAS NMR spectra of (a) HZSM5-11.5 after exposure to 50 pulses of water, (b) fresh HZSM5-11.5, and HZSM5−11.5 treated by steaming for (c) 0.5 h and (d) 3 h.

indicate a qualitative increased presence of Al species that are not traditional framework sites upon high-temperature water treatment, a subset of which correlates to enhancements in activity for hexane cracking at elevated temperatures. It is noted that, in comparison to the activity of the 0.5 h steaming sample, a significant loss in activity was observed for the 3 h steaming sample with a comparable loss of Brønsted sites. This indicates that the number of synergistic sites was reduced due to the loss of the Brønsted sites or/and active EFAL corresponding to these sites during steaming. Water may interact with and assist in the mobility of EFAL species to form more stable Al_2O_3 clusters at longer steaming times.

3.3.2. Implications on Catalytic Activity by Pulsing Water. Since pulsing water does not lead to significant dealumination, which decreases the number of Brønsted acid sites and ultimately collapses the zeolite structure, this method is crucial to evaluate the change in catalytic activity by water vapor without the convoluted effects of modified zeolite pores or collapse of the crystal. Figure 6 shows the change in reactivity of various HZSM-5 catalysts as a function of sequential pulses of water. It is observed that water pulses have the greatest positive influence on reactivity for HZSM5-11.5 and HZSM5-15, which have higher BAS densities and significant amounts of AlOH species that are not from the framework BAS in their parent structure. In addition, HZSM5-15 and HZSM5-15-AHFS have the same BAS density and distribution of sites but only a slight activity enhancement by the water treatment is observed on the catalyst HZSM5-15-AHFS, where most of the EFAL species were removed. This evidence suggests that water is interacting with existing EFAL species to create new sites with enhanced catalytic activity during the pulsing water treatments. For the same reason, the low concentration of EFAL species in HZSM5-40 leads to a lower possibility to form the synergistic sites; therefore, significant rate enhancements are not observed in this catalyst upon pulsed water treatments. In the case of HZSM5-25, a high activity per proton in the parent zeolite is observed while pulsing water

https://doi.org/10.1021/acscatal.1c01138
ACS Catal. 2021, 11, 6982−6994

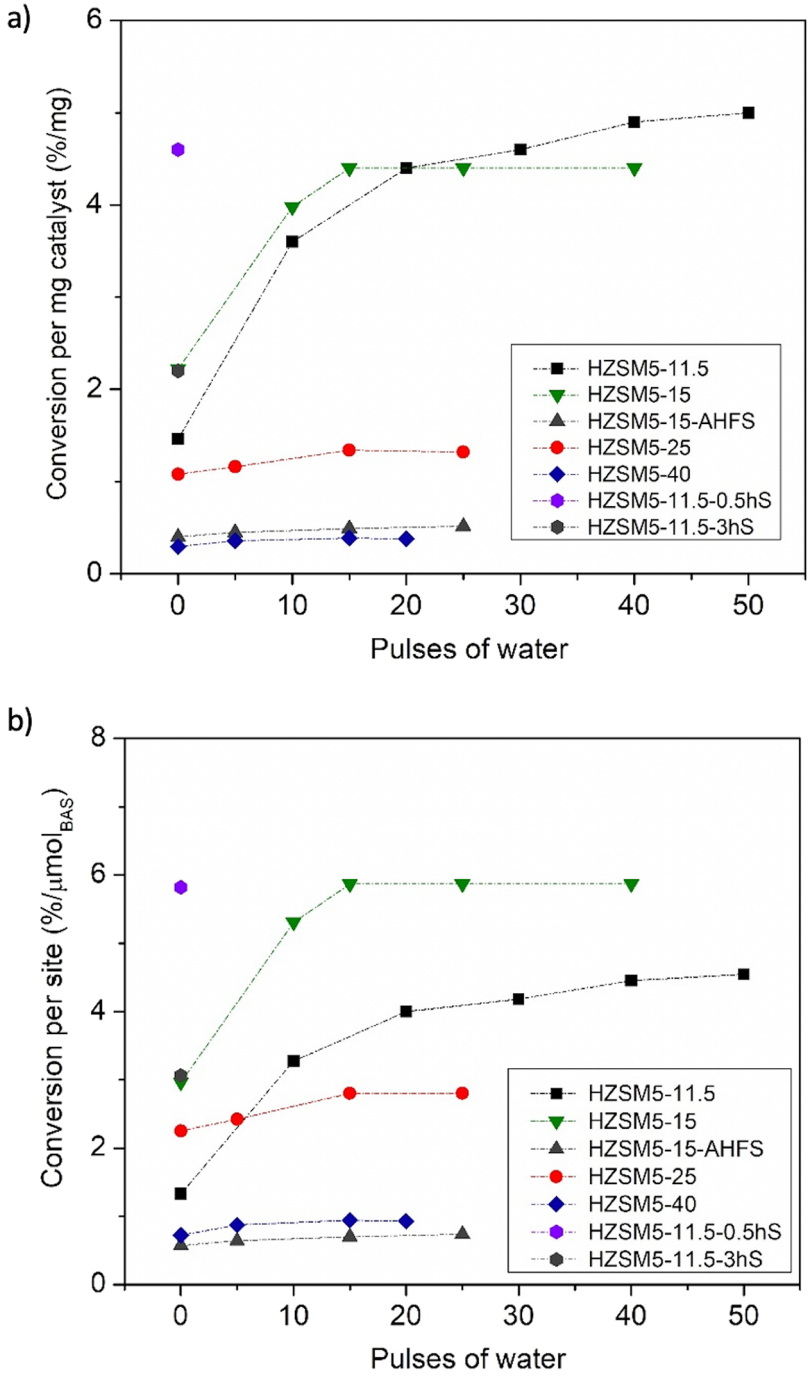

Figure 6. Conversion normalized by (a) the amount of utilized catalyst and (b) the number of mol_{BAS} of various HZSM-5 zeolites as a function of pulses of water treatment. Reaction conditions: T = 480 °C, P_{nC6} = 4.5 kPa, amount of catalysts varied to achieve initial conversions within 5−15%. A diagram of the pulse experiment is given in Figure S3.

treatment does not lead to pronounced enhancements in the reactivity of this catalyst, although the concentration of EFAL species and BAS density of this catalyst are relatively high. This implies that other factors such as the number of BAS-BAS pairs, the form of EFAL species, etc. likely play an important role in the formation of synergistic sites.

In summary, under this condition of pulsing treatment, water does not lead to further dealumination of the zeolite framework but likely interacts with existing EFAL species to improve their rate of migration. These EFAL species are possibly mobile until they are kinetically trapped at stable positions closed to framework BAS to form synergistic sites. It is well-known that severe steaming for longer times can facilitate further migration of EFAL species to form Al_2O_3 clusters, but we hypothesize that the steam contact time required for this degree of migration is far greater than that observed in the presence of these pulses. These sites are stable under the treatment conditions used, and the activity likely remains once it reaches the maximum. We hypothesize that the Brønsted/Brønsted pair sites might help to stabilize the EFAL species and kinetically trap these species.

https://doi.org/10.1021/acscatal.1c01138
ACS Catal. 2021, 11, 6982−6994

The strong inhibition of cracking rate is observed when the HZSM5-11.5 catalyst is exposed to 50 sequential pulses of water, as shown in Figure 7. The catalyst is exposed to only

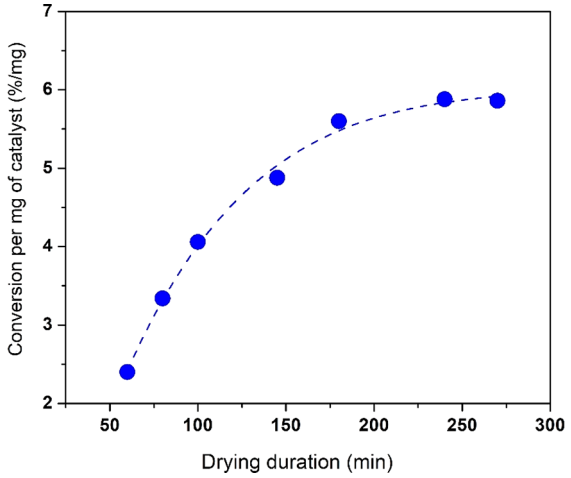

Figure 7. Effect of drying duration after the catalyst HZSM5-11.5 was exposed to 50 sequential pulses of water. Water treatment conditions: T = 480 °C, water partial pressure of 18.6 kPa and 2.85 μmol of water in each pulse. Cracking reaction conditions: T = 480 °C, P_{nC6} = 4.5 kPa with 0.48 μmol of n-hexane injected in each pulse, 5 mg of catalyst.

2.85 μmol of water in each pulse at high temperature, 480 °C, and the contact time between the catalyst and water is very short in the pulsing treatment. However, the drying time to reach the maximum activity is up to 6 h. Since the activity of synergistic sites is much higher in comparison to that of traditional sites, the change in activity is strongly affected by the number of these sites. This strong inhibition of the rate might be explained by the absorption of water on the synergistic sites or the interaction of water with EFAL species belonging to these highly active sites. As the interconversion of various EFAL species happens inside the zeolite in the presence of water,[52] water likely converts EFAL species into their "inactive" hydrated forms, possibly to generate AlOH species. The dehydration of these species and removal of residual moisture are energetically demanding, as evidenced by the prolonged needed thermal treatment at high temperature to recover the activity. Note that it is difficult to decouple the dehydration of EFAL species from their migration during the drying process, since we believe both happen concurrently. Under more severe steaming treatments, the measured activity might be significantly influenced by the presence of water. This might help to explain some of the contradictory claims in the literature regarding the catalytic role of created sites.

3.3.3. Generating EFAL Species by Steaming. Dealumination leading to the generation of additional EFAL can occur under continuous steaming conditions. Table 2 gives the steaming conditions investigated for several catalysts that exhibit no activity enhancement by simply pulsing water. The water partial pressures used in the steaming treatments shown in Table 2 were lower in comparison to the conditions used in the pulsing treatment to minimize the rate of modification to the framework.

When an alternative framework of TON, HZSM22, which has 10-membered rings without the intersections present in HZSM5 catalysts, is considered, the influence of site location may be evaluated. It should be noted that, while HZSM22 exhibits the same number of T sites per ring, the shape of the opening is mildly compressed, so while confinement effects induced by MFI straight or zigzag channels cannot be compared exactly, they do serve as surrogates to determine the influence that confinement in general plays on these rates. Interestingly, the rate per BAS for the fresh HZSM-22 catalyst is comparable to that observed over HZSM5 with a Si/Al ratio of 140, where we would anticipate the majority of active sites are present in the channel intersections.[44] Further, higher steam partial pressures were required to significantly create EFAL sites in the HZSM-22 catalyst. Interestingly, the rate per proton did not vary, indicating both that the reaction appears to not be influenced by internal diffusion and that the local environment of the EFAL species alone does not fully describe the observed rate in catalysts with low framework Al density under these conditions. Rather, it reinforces the concept that framework sites in close proximity are required to generate these synergistic active sites.

Another interesting yet expected observation is the correlation between framework site density and the resulting rate of dealumination. This is most pronounced for the Si/Al 140 MFI catalyst, where no significant reduction in BAS density is observed after a steam treatment that is far more severe than the treatment that the MFI catalysts with higher site densities were exposed to. This is in line with the diminished rate of BAS loss with prolonged steaming time as the framework acid site density decreases with time, as shown in Figure 3 and in agreement with general practices for other zeolite families, such as USY zeolites commonly employed for catalytic cracking.

3.4. Estimation of Activity and Number of Active Acid Sites. The rate and activation energy associated with synergistic sites can be calculated on the basis of the observed n-hexane cracking activity. This is accomplished by simply

Table 2. Steaming Conditions and the Changes in Catalytic Activity Measured by the Conversion of n-Hexane Cracking of Zeolite Samples

		steaming conditions			conversion per mg catalyst (%/mg)	
sample	conversion per site of fresh catalyst (%/μmol$_{BAS}$)	duration (h)	temp (°C)	pressure (kPa)	fresh zeolite	steamed zeolite
HZSM5-40	0.73	4	480	10	0.29	0.51
HZSM5-15-AHFS	0.65	4	480	10	0.46	1.38
HZSM-22	0.45	10	480	10	0.14	0.14
		4	480	18.6	0.14	0.11[a]
HZSM5-140	0.44	4	480	18.6	0.044	0.044

[a]The BAS density of HZSM-22 after 4 h of steaming at 18.6 kPa of water vapor is 0.26 mmol/g.

https://doi.org/10.1021/acscatal.1c01138
ACS Catal. 2021, 11, 6982−6994

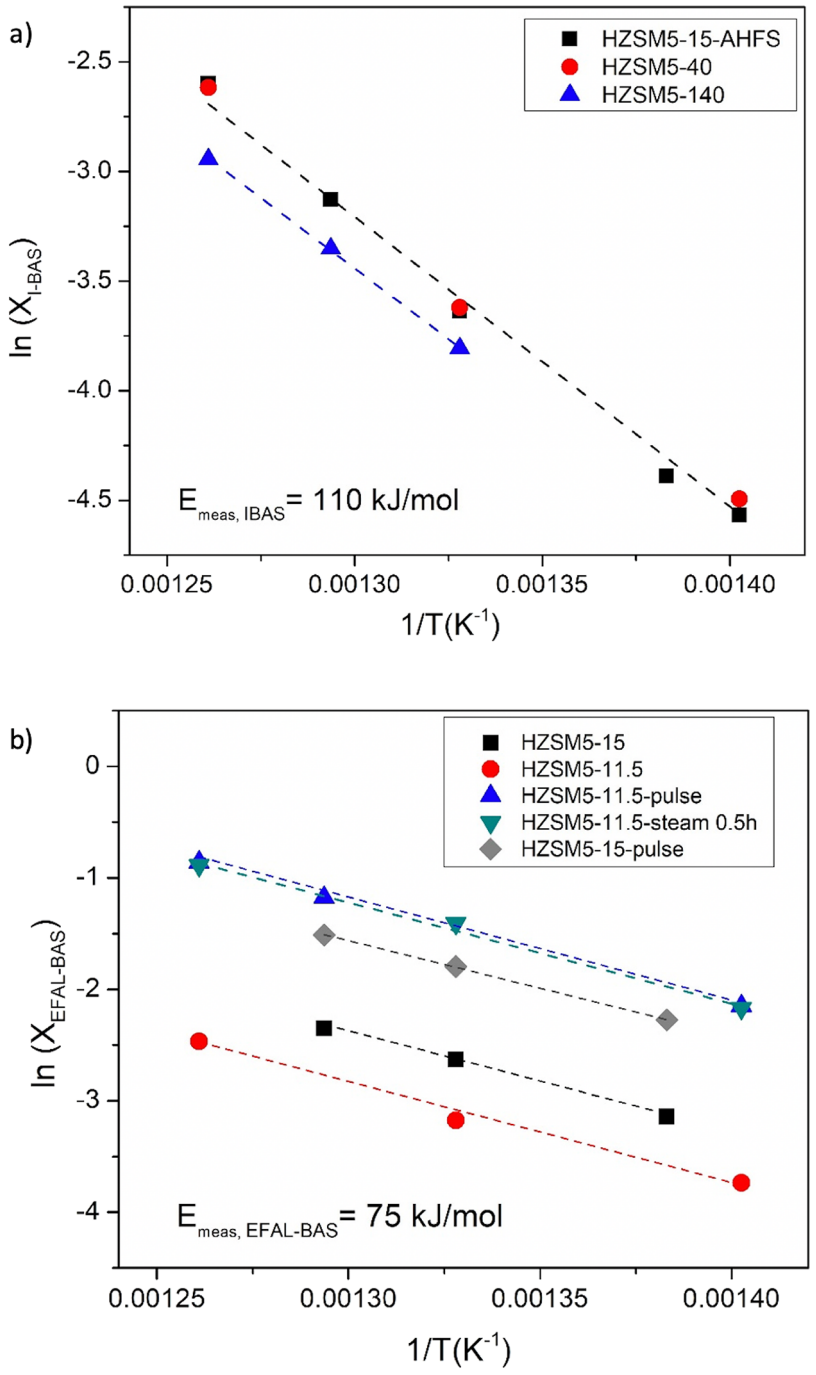

Figure 8. Arrhenius plot of depicting conversion versus inverse temperature on (a) isolated Brønsted acid sites and (b) synergistic EFAL-BAS sites. Reaction conditions: T = 440−520 °C, P_{nC6} = 4.5 kPa, amount of catalysts varied to achieve conversions within 5−15%.

estimating the activity per isolated Brønsted acid site and determining the activity resulting from a synergistic active site. This is accomplished by the following:

$$\begin{aligned}\bar{X}_{\text{total}} &= \bar{X}_{\text{I-BAS}} + \bar{X}_{\text{EFAL-BAS}} \\ &= N_{\text{I-BAS}}X'_{\text{I-BAS}} + N_{\text{EFAL-BAS}}X'_{\text{EFAL-BAS}} \\ \bar{X}_{\text{total}} &= (N_{\text{BAS-total}} - N_{\text{EFAL-BAS}})X'_{I-BAS} \\ &\quad + N_{\text{EFAL-BAS}}X'_{\text{EFAL-BAS}} \end{aligned} \quad (1)$$

where $\bar{X}_{\text{total}}$, $\bar{\bar{X}}_{\text{I-BAS}}$, and $\bar{\bar{X}}_{\text{EFAL-BAS}}$ are the conversions associated with each site per milligram of catalyst (%/mg), $X'_{\text{I-BAS}}$ and $X'_{\text{EFAL-BAS}}$ are the conversions per site (%/μmol), and $N_{\text{BAS-total}}$, $N_{\text{I-BAS}}$, $N_{\text{EFAL-BAS}}$ are the number of total Brønsted sites, isolated Brønsted sites, and synergistic sites per milligram, respectively (mmol/g). Since the activity of a synergistic site is much higher than that of an isolated BAS ($X'_{\text{EFAL-BAS}}/X'_{\text{I-BAS}}$ = 52 ± 2, reported by Zhang et al.[18]) and the fraction of EFAL-BAS sites is small, the term $X'_{\text{I-BAS}}N_{\text{EFAL-BAS}}$ is negligible. The conversion attributed to the synergistic sites can be calculated from eq 1 as

$$\bar{X}_{\text{EFAL-BAS}} = N_{\text{EFAL-BAS}}X'_{\text{EFAL-BAS}} = \bar{X}_{\text{total}} - N_{\text{BAS-total}}X'_{\text{I-BAS}} \quad (2)$$

in which $X'_{\text{I-BAS}}$ was determined by the conversion per μmol of BAS sites on HZSM5-15-AHFS at the corresponding reaction

https://doi.org/10.1021/acscatal.1c01138
ACS Catal. 2021, 11, 6982−6994

temperature. On the assumption that the activities of synergistic sites in all HZSM-5 catalysts are similar, the value $\overline{X}_{\text{EFAL-BAS}}$ is proportional to the number of these sites in the catalysts and represents the rate of the reaction corresponding to the synergistic sites.

^{1}H MAS NMR might be utilized to determine the number of different proton species. HZSM5-15 and HZSM5-15-AHFS catalysts in this section are identical with those used by Chen et al.[7] Table S2 gives the distribution of H species from ^{1}H MAS NMR of two catalyst samples adapted from that study. If one assumes that the 12−15 ppm peak corresponds to the synergistic sites,[7] the number of synergistic sites in HZSM5-15, $N_{\text{EFAL-BAS}}$, is estimated as 0.059 mmol/g. At 480 °C, $X'_{\text{I-BAS}}$ = 0.65%/μmol was estimated by the conversion of the reaction on HZSM5-15-AHFS and the value of the activity on the synergistic sites, X spm'$_{\text{EFAL-BAS}}$, estimated from eqs 1 is 32.2%/μmol. Once the values of $X'_{\text{I-BAS}}$, $X'_{\text{EFAL-BAS}}$, and $\overline{X}_{\text{total}}$ were known at 480 °C, the number of synergistic sites of given catalyst could be calculated by eq 1. We note that quantifying the small number of synergistic sites can be challenging, especially for the samples after exposure to water treatment. Any uncertainty in this value due to additional species overlapping within the 12−15 ppm peak could result in overestimations in site counting. Similarly, any additional peaks that are not considered could lead to underestimations in site counting. Regardless, the number of synergistic sites is a small fraction of the total Brønsted sites present in the zeolite and, critically for this exercise, the activation energy values attributed to these sites as well as to their creation will still be accurate.

3.5. Activation Energy of *n*-Hexane Cracking Reaction. The turnover rates of the first-order reaction at low coverage are given by

$$\text{rate} = k_{\text{int}} C_{\text{A(z)}} = k_{\text{int}} K_{\text{ads}} P_{\text{A}} = k_{\text{meas}} P_{\text{A}}$$

with $C_{\text{A(z)}}$ indicating the surface concentration of adsorbed alkanes. P_{A} is the alkane partial pressure, k is the cracking rate constant, and K_{ads} is the equilibrium constant of alkane adsorption.

The intrinsic activation energies (E_{int}) can be calculated from these measured activation energies (E_{meas}) and the enthalpies of adsorption as follows:

$$E_{\text{int}} = E_{\text{meas}} - \Delta H_{\text{ads}}$$

Since the rate of the reaction is proportional to the conversion of the pulse, the Arrhenius plots of the natural logarithm of conversion of reaction as a function of inverse temperature are reported to determine the activation energy of *n*-hexane cracking on synergistic sites and isolated sites (Figure 8). The activation energy of ∼110 kJ/mol was measured on isolated BAS sites utilizing catalysts with an insignificant number of synergistic sites: HZSM5-15-AHFS, HZSM5-40, and HZSM5-140. This barrier is comparable to those reported in reported in refs 53 and 54. Meanwhile, the rate attributed to synergistic sites was calculated by subtracting the rate observed at different temperatures corresponding to isolated sites (eq 2). Remarkably, regardless of the Si/Al ratio or subsequent treatments employed, the apparent energy barriers observed over the synergistic sites were quite similar: ∼75 kJ/mol. The results show that the enhancement in activity is due to the increase in the number of generated active sites, while the intrinsic activity of the synergistic site is not altered. This identical observed barrier also suggests that the reaction rates are not corrupted by internal or external diffusion even at the highest rate per catalyst particle. Iglesia and others have attributed activity enhancements to modifications to the local confining environment surrounding the active site for a variety of reactions.[21,55] In this particular case, an EFAL species in proximity to a framework Brønsted site may modify the local confinement of the transition state. Regardless of the nature of activity enhancement, by stabilization of kinetically relevant transition states or by enhancing adsorption of reactive intermediates, the nature of the enhanced sites to lower the apparent enthalpy of reaction appears to be consistent across a wide range of catalysts studied. Alternative proposals, such as the suggestion that enhancements due to synergistic sites are simply due to modifications in transition state entropies,[18] appear to not fully explain the behavior observed here for this reaction in question, as a clear shift in apparent activation enthalpy is observed. Further studies are necessary to determine how EFAL species manipulate the adsorbed intermediates and transition states leading to these remarkable rate enhancements.

3.6. Activation Energy of Generation of Synergistic Sites. Prior to inferring site generation details, we clarify our hypothesis regarding the nature of the synergistic sites in question. Many arguments have been made regarding the nature of active sites within zeolite pores. These arguments are confounded by the fact that certain surface features may be highly active for specific reactions of interest. All arguments proposed here correlate with sites responsible for *n*-alkane cracking. Differences in activity have been reported for various T site locations within MFI crystals, such as within intersections vs pore channels, for some families of reactions.[22] In the cases reported here for *n*-alkane activation, however, activity enhancements are observed without perturbing total site density. Sites responsible for observed rate enhancements cannot be due to modifications in T site location but migration of more mobile species. We have also reported previously the intriguing role of partially coordinated species for more facile reactions.[8] It is important to note here that, while partially coordinated sites are likely responsible for some chemistry, their presence can shift on the basis of interaction with heteroatoms such as moisture, and some have speculated that at the high temperatures required for more demanding hydrocarbon chemistry these features may no longer exist.[25,26] Supportive of such an argument is the fact that the synergistic active sites in question here are only apparent after extended drying periods under elevated temperature conditions (Figure 7). Furthermore, if these sites are created in the HZSM5-15 parent during a pulsing water treatment, they should be formed in AHFS-washed HZSM5−15 catalyst as well. However, the fact that we did not observe the rate enhancement when we exposed AHFS-washed HZSM5-15 catalyst to pulses of water suggests that the partially coordinated sites, if they are formed under the pulsed treatments in question, are not responsible for the reaction rate enhancement. Further, the barrier that was quantified for the creation of these sites is more typical of EFAL migration than of full framework hydrolysis, which generally requires much larger activation energies.[45] We are careful to note, however, that these partially coordinated species may be precursors to the extra-lattice species required for alkane cracking rate enhancements. Therefore, we hypothesize that the role of water under these conditions is simply to accelerate the formation of these synergistic sites via the migration of

https://doi.org/10.1021/acscatal.1c01138
ACS Catal. 2021, 11, 6982−6994

existing extra-framework species, and the pulse reactor employed here allows the direct quantification of activation barriers associated with this migration.

To estimate the energy barrier of this process, the activity of various HZSM-5-11.5 samples after treatment at different temperatures was measured while the partial pressure of water in the pulse, residence time, and all other conditions remained constant. A significant number of 40 pulses of water with a break of 10 min intervals between pulses was utilized in all cases to observe significant differences in the activity for the treated catalysts. After water treatment, the temperature of the reactor was raised to 480 °C to dry catalysts for 10 h and we carried out an *n*-hexane cracking reaction to test the activity of the catalyst. The conversion of this reaction was utilized to estimate the activity of active sites. The activation energy associated with the generation of synergistic sites as shown in Figure 9 is 44 kJ/mol, corresponding to the rate of new

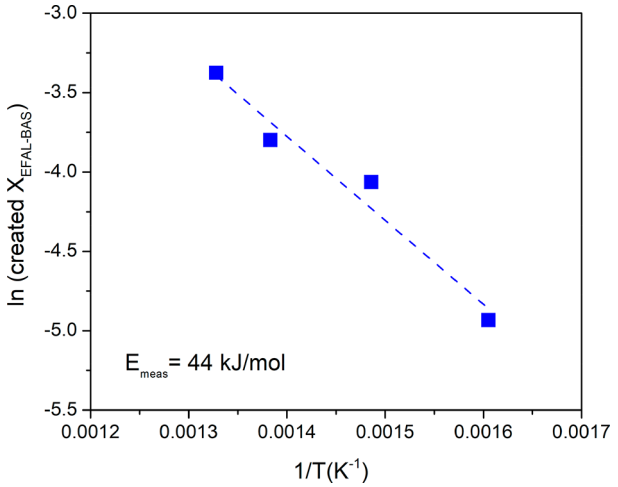

Figure 9. Arrhenius plot of depicting conversion by created synergistic site versus inverse water treatment temperature on HZSM5-11.5.

synergistic site generation as discussed above. This value is comparable with the energy barrier of the stepwise immigration of the partially dehydrated $[Al(OH)_2]^+$ cation along the supercage in Faujasite zeolite estimated by DFT.[52] In addition, this barrier is significantly lower than predicted barriers reported for dealumination of a framework site. A relatively high energy barrier, E_{act} = 190 kJ/mol, has been reported for dealumination of HZSM-5 zeolites by Silaghi et al.[45]

To further investigate the migration of extra-framework $[Al(OH)_2]^+$ between different locations in MFI zeolites, the activation barriers and reaction energies associated with the migration of $[Al(OH)_2]^+$ at the intersection were calculated (Figure 10). The migration of $[Al(OH)_2]^+$ at the intersection is affected by electrostatic interactions between the positively charged EFAL and the negative charge around the framework Al. That is, the framework Al exerts electrostatic force on the $[Al(OH)_2]^+$ cation and attracts it to move closer to the framework Al. The $[Al(OH)_2]^+$ cation prefers a location facing to the framework Al even though there is a spacer of a −O−Si−O− unit between them in the structure shown in Figure 10. The migration of $[Al(OH)_2]^+$ to a farther location that is away from the framework Al by one more unit of −O−Si−O− is endothermic by 29−36 kJ/mol with an activation barrier of

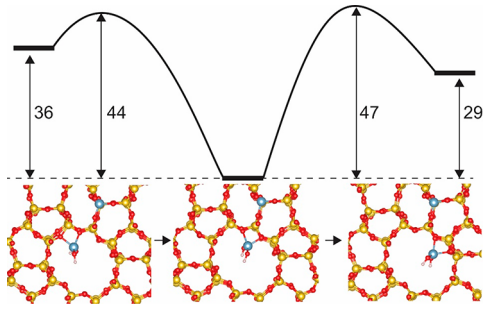

Figure 10. DFT calculations of $Al(OH)_2^+$ migration at the intersection of HZSM-5. One framework Al was introduced to balance the charge. The Al, Si, O, and H atoms are shown in blue, yellow, red, and white, respectively. The units in the energy profile are kJ/mol.

44−47 kJ/mol. In other words, for $[Al(OH)_2]^+$ that is farther away from the framework Al, there is a driving force for it to migrate toward the framework Al due to the enhanced stability, with an moderate activation barrier of 9−18 kJ/mol. The migration of $[Al(OH)_2]^+$ in the sinusoidal channel was also examined. The $[Al(OH)_2]^+$ was intentionally positioned far from the framework Al to reduce the effects of electrostatic interactions. The results indicate that the migration of $[Al(OH)_2]^+$ from a location close to a T12 site to one close to a T3 site in the sinusoidal channel is a thermodynamically neutral process (ΔE = 2 kJ/mol) and the calculated activation energy is 23 kJ/mol. These calculations thus suggest the barrier associated with the migration of the EFAL cation is moderate and the migration dynamics are driven toward framework Al species, with barriers associated with migration away from local minima to more preferentially stabilized locations, likely pairs of sites, corresponding to barriers consistent with those observed experimentally.

4. CONCLUSION

The use of a micropulse reactor to decouple EFAL migration from framework hydrolysis is a revealing way to evaluate the creation of new sites with enhanced activity. The various micropulse treatment conditions employed and further evaluated for *n*-hexane cracking over HZSM-5 zeolites when they are contrasted with continuous steam treatments illustrate the that the important role of water is not only site generation through hydrolysis but also the subsequent Al migration to form metastable synergistic sites prior to Al_2O_3 cluster formation. During continuous steaming, dealumination converts framework aluminum to EFAL species, which is helpful for enhancing the catalytic activity of a catalyst having a low BAS density or a low concentration of EFAL species. The activity of catalysts having lower BAS density such as HZSM5-140 could not be enhanced under the treatment condition by both methods, indicating that not only the presence of EFAL but also the density of framework sites is important. We hypothesize that this is necessary to stabilize EFAL species in the proximity of an adjacent BAS to create the synergistic sites. The micropulse experiments suggest that water enhances the mobility of EFAL species to create synergistic sites. By quantifying strong BAS density as well as *n*-hexane cracking activity per site, the activation energy associated with the newly created sites as well as the rate of their creation can be quantified and distinguished from framework dealumination. The apparent activation energy of hexane cracking over

https://doi.org/10.1021/acscatal.1c01138
ACS Catal. 2021, 11, 6982−6994

synergistic sites is ∼75 kJ/mol across all catalysts studied, which is significantly lower than the barrier observed over traditional BAS, ∼110 kJ/mol. In addition, the energy barrier associated with the creation of new synergistic sites in the presence of water pulses, or the migration of Al, was found to be 44 kJ/mol, far lower than the barrier required for framework dealumination but an essential step for further activity enhancement of cracking activity.

■ ASSOCIATED CONTENT

Supporting Information

The Supporting Information is available free of charge at https://pubs.acs.org/doi/10.1021/acscatal.1c01138.

Determination of the order of the reaction, shapes of the pulses with different partial pressures of *n*-hexane, product distribution as a function of conversion level of the *n*-hexane cracking reaction on HZSM5-11.5 zeolite, product distribution of the *n*-hexane cracking reaction on HZSM5-11.5 zeolite at the same level of conversion, diagram of pulse experiment, surface area and pore volume of ZSM5-11.5 samples, and distribution of species from ^{1}H MAS NMR spectra of the HZSM-5 catalysts (PDF)

■ AUTHOR INFORMATION

Corresponding Author

Steven Crossley − *School of Chemical, Biological, and Materials Engineering, University of Oklahoma, Norman, Oklahoma 73019, United States;* orcid.org/0000-0002-1017-9839; Email: stevencrossley@ou.edu

Authors

Tram N. Pham − *School of Chemical, Biological, and Materials Engineering, University of Oklahoma, Norman, Oklahoma 73019, United States*

Vy Nguyen − *School of Chemical, Biological, and Materials Engineering, University of Oklahoma, Norman, Oklahoma 73019, United States*

Bin Wang − *School of Chemical, Biological, and Materials Engineering, University of Oklahoma, Norman, Oklahoma 73019, United States;* orcid.org/0000-0001-8246-1422

Jeffery L. White − *School of Chemical Engineering, Oklahoma State University, Stillwater, Oklahoma 74078, United States;* orcid.org/0000-0003-4065-321X

Complete contact information is available at: https://pubs.acs.org/10.1021/acscatal.1c01138

Notes

The authors declare no competing financial interest.

■ ACKNOWLEDGMENTS

This material is based upon work supported by the National Science Foundation under Grant Nos. CHE-1764116 and CHE-1764130, whose support is gratefully acknowledged. The DFT calculations were performed using computational resources at the OU Supercomputing Center for Education & Research (OSCER) at the University of Oklahoma.

■ REFERENCES

(1) Derouane, E. G.; Védrine, J. C.; Pinto, R. R.; Borges, P. M.; Costa, L.; Lemos, M. A. N. D. A.; Lemos, F.; Ribeiro, F. R. The Acidity of Zeolites: Concepts, Measurements and Relation to Catalysis: A Review on Experimental and Theoretical Methods for the Study of Zeolite Acidity. *Catal. Rev.: Sci. Eng.* **2013**, *55* (4), 454−515.

(2) Resasco, D. E.; Wang, B.; Crossley, S. Zeolite-catalysed C-C bond forming reactions for biomass conversion to fuels and chemicals. *Catal. Sci. Technol.* **2016**, *6* (8), 2543−2559.

(3) Derouane, E. G.; Andre, J.-M.; Lucas, A. A. Surface curvature effects in physisorption and catalysis by microporous solids and molecular sieves. *J. Catal.* **1988**, *110* (1), 58−73.

(4) Noh, G.; Shi, Z.; Zones, S. I.; Iglesia, E. Isomerization and *β*-scission reactions of alkanes on bifunctional metal-acid catalysts: Consequences of confinement and diffusional constraints on reactivity and selectivity. *J. Catal.* **2018**, *368*, 389−410.

(5) Gorte, R. J.; Crossley, S. P. A perspective on catalysis in solid acids. *J. Catal.* **2019**, *375*, 524−530.

(6) Crossley, S. P.; Resasco, D. E.; Haller, G. L. Clarifying the multiple roles of confinement in zeolites: From stabilization of transition states to modification of internal diffusion rates. *J. Catal.* **2019**, *372*, 382−387.

(7) Chen, K.; Abdolrahmani, M.; Horstmeier, S.; Pham, T. N.; Nguyen, V. T.; Zeets, M.; Wang, B.; Crossley, S.; White, J. L. Brønsted-Brønsted Synergies between Framework and Noncrystalline Protons in Zeolite H-ZSM-5. *ACS Catal.* **2019**, *9*, 6124−6136.

(8) Chen, K.; Horstmeier, S.; Nguyen, V. T.; Wang, B.; Crossley, S. P.; Pham, T.; Gan, Z.; Hung, I.; White, J. L. Structure and Catalytic Characterization of a Second Framework Al(IV) Site in Zeolite Catalysts Revealed by NMR at 35.2 T. *J. Am. Chem. Soc.* **2020**, *142* (16), 7514−7523.

(9) Kung, H. H.; Williams, B. A.; Babitz, S. M.; Miller, J. T.; Haag, W. O.; Snurr, R. Q. Enhanced hydrocarbon cracking activity of Y zeolites. *Top. Catal.* **2000**, *10* (1), 59−64.

(10) Werner, O.; Haag, L.; Rudolph, M. Enhancement of zeolite catalytic activity. US-0121339, 1982.

(11) Masuda, T.; Fujikata, Y.; Mukai, S. R.; Hashimoto, K. Changes in catalytic activity of MFI-type zeolites caused by dealumination in a steam atmosphere. *Appl. Catal., A* **1998**, *172* (1), 73−83.

(12) Ristanović, Z.; Hofmann, J. P.; De Cremer, G.; Kubarev, A. V.; Rohnke, M.; Meirer, F.; Hofkens, J.; Roeffaers, M. B. J.; Weckhuysen, B. M. Quantitative 3D Fluorescence Imaging of Single Catalytic Turnovers Reveals Spatiotemporal Gradients in Reactivity of Zeolite H-ZSM-5 Crystals upon Steaming. *J. Am. Chem. Soc.* **2015**, *137* (20), 6559−6568.

(13) Niwa, M.; Sota, S.; Katada, N. Strong Brønsted acid site in HZSM-5 created by mild steaming. *Catal. Today* **2012**, *185* (1), 17−24.

(14) van Bokhoven, J. A.; Tromp, M.; Koningsberger, D. C.; Miller, J. T.; Pieterse, J. A. Z.; Lercher, J. A.; Williams, B. A.; Kung, H. H. An Explanation for the Enhanced Activity for Light Alkane Conversion in Mildly Steam Dealuminated Mordenite: The Dominant Role of Adsorption. *J. Catal.* **2001**, *202* (1), 129−140.

(15) Zholobenko, V. L.; Kustov, L. M.; Kazansky, V. B.; Loeffler, E.; Lohser, U.; Peuker, C.; Oehlmann, G. On the possible nature of sites responsible for the enhancement of cracking activity of HZSM-5 zeolites dealuminated under mild steaming conditions. *Zeolites* **1990**, *10* (4), 304−306.

(16) Schallmoser, S.; Ikuno, T.; Wagenhofer, M. F.; Kolvenbach, R.; Haller, G. L.; Sanchez-Sanchez, M.; Lercher, J. A. Impact of the local environment of Brønsted acid sites in ZSM-5 on the catalytic activity in n-pentane cracking. *J. Catal.* **2014**, *316*, 93−102.

(17) Li, S.; Zheng, A.; Su, Y.; Zhang, H.; Chen, L.; Yang, J.; Ye, C.; Deng, F. Brønsted/Lewis Acid Synergy in Dealuminated HY Zeolite: A Combined Solid-State NMR and Theoretical Calculation Study. *J. Am. Chem. Soc.* **2007**, *129* (36), 11161−11171.

(18) Zhang, Y.; Zhao, R.; Sanchez-Sanchez, M.; Haller, G. L.; Hu, J.; Bermejo-Deval, R.; Liu, Y.; Lercher, J. A. Promotion of protolytic pentane conversion on H-MFI zeolite by proximity of extra-framework aluminum oxide and Brønsted acid sites. *J. Catal.* **2019**, *370*, 424−433.

(19) Maier, S. M.; Jentys, A.; Lercher, J. A. Steaming of Zeolite BEA and Its Effect on Acidity: A Comparative NMR and IR Spectroscopic Study. *J. Phys. Chem. C* **2011**, *115* (16), 8005−8013.
(20) Gounder, R.; Jones, A. J.; Carr, R. T.; Iglesia, E. Solvation and acid strength effects on catalysis by faujasite zeolites. *J. Catal.* **2012**, *286*, 214−223.
(21) Gounder, R.; Iglesia, E. The catalytic diversity of zeolites: confinement and solvation effects within voids of molecular dimensions. *Chem. Commun.* **2013**, *49* (34), 3491−3509.
(22) Jones, A. J.; Iglesia, E. The Strength of Brønsted Acid Sites in Microporous Aluminosilicates. *ACS Catal.* **2015**, *5* (10), 5741−5755.
(23) Abdolrahmani, M.; Chen, K.; White, J. L. Assessment, Control, and Impact of Brønsted Acid Site Heterogeneity in Zeolite HZSM-5. *J. Phys. Chem. C* **2018**, *122* (27), 15520−15528.
(24) Chen, K.; Abdolrhamani, M.; Sheets, E.; Freeman, J.; Ward, G.; White, J. L. Direct Detection of Multiple Acidic Proton Sites in Zeolite HZSM-5. *J. Am. Chem. Soc.* **2017**, *139* (51), 18698−18704.
(25) Omegna, A.; Prins, R.; van Bokhoven, J. A. Effect of Temperature on Aluminum Coordination in Zeolites H-Y and H-USY and Amorphous Silica-Alumina: An in Situ Al K Edge XANES Study. *J. Phys. Chem. B* **2005**, *109* (19), 9280−9283.
(26) Omegna, A.; van Bokhoven, J. A.; Prins, R. Flexible Aluminum Coordination in Alumino-Silicates. Structure of Zeolite H-USY and Amorphous Silica-Alumina. *J. Phys. Chem. B* **2003**, *107*, 8854−8860.
(27) van Bokhoven, J. A.; Williams, B. A.; Ji, W.; Koningsberger, D. C.; Kung, H. H.; Miller, J. T. Observation of a compensation relation for monomolecular alkane cracking by zeolites: the dominant role of reactant sorption. *J. Catal.* **2004**, *224* (1), 50−59.
(28) Janda, A.; Bell, A. T. Effects of Si/Al Ratio on the Distribution of Framework Al and on the Rates of Alkane Monomolecular Cracking and Dehydrogenation in H-MFI. *J. Am. Chem. Soc.* **2013**, *135* (51), 19193−19207.
(29) Weisz, P. B.; Miale, J. N. Superactive crystalline aluminosilicate hydrocarbon catalysts. *J. Catal.* **1965**, *4* (4), 527−529.
(30) Miale, J. N.; Chen, N. Y.; Weisz, P. B. Catalysis by crystalline aluminosilicates: IV. Attainable catalytic cracking rate constants, and superactivity. *J. Catal.* **1966**, *6* (2), 278−287.
(31) Olson, D. H.; Haag, W. O.; Lago, R. M. Chemical and physical properties of the ZSM-5 substitutional series. *J. Catal.* **1980**, *61* (2), 390−396.
(32) Haag, W. O.; Lago, R. M.; Weisz, P. B. The active site of acidic aluminosilicate catalysts. *Nature* **1984**, *309* (5969), 589−591.
(33) Garralón, G.; Fornés, V.; Corma, A. Faujasites dealuminated with ammonium hexafluorosilicate: Variables affecting the method of preparation. *Zeolites* **1988**, *8* (4), 268−272.
(34) Kresse, G.; Furthmuller, J. Efficient iterative schemes for ab initio total-energy calculations using a plane-wave basis set. *Phys. Rev. B: Condens. Matter Mater. Phys.* **1996**, *54* (16), 11169−11186.
(35) Kresse, G.; Joubert, D. From ultrasoft pseudopotentials to the projector augmented-wave method. *Phys. Rev. B: Condens. Matter Mater. Phys.* **1999**, *59* (3), 1758−1775.
(36) Blochl, P. E. Projector Augmented-Wave Method. *Phys. Rev. B: Condens. Matter Mater. Phys.* **1994**, *50* (24), 17953−17979.
(37) Perdew, J. P.; Burke, K.; Ernzerhof, M. Generalized gradient approximation made simple. *Phys. Rev. Lett.* **1996**, *77* (18), 3865−3868.
(38) Grimme, S.; Antony, J.; Ehrlich, S.; Krieg, H. A consistent and accurate ab initio parametrization of density functional dispersion correction (DFT-D) for the 94 elements H-Pu. *J. Chem. Phys.* **2010**, *132* (15), 154104.
(39) Zeets, M.; Resasco, D. E.; Wang, B. Enhanced chemical activity and wettability at adjacent Brønsted acid sites in HZSM-5. *Catal. Today* **2018**, *312*, 44−50.
(40) Henkelman, G.; Uberuaga, B. P.; Jonsson, H. A climbing image nudged elastic band method for finding saddle points and minimum energy paths. *J. Chem. Phys.* **2000**, *113* (22), 9901−9904.
(41) Sica, A. M.; Valles, E. M.; Gigola, C. E. Kinetic Data form a Pulse Microcatalytic Reactor-Hydrogenation of Benzene on a Nickel Catalyst. *J. Catal.* **1978**, *51*, 115−125.
(42) Attar, A. Pulsed differential reactors and their use for kinetic studies of gas-solid reactions—application to mechanistic studies of the reactions of hydrogen sulfide and the alkaline minerals in coal. *Rev. Sci. Instrum.* **1979**, *50* (1), 111−117.
(43) Babitz, S. M.; Williams, B. A.; Miller, J. T.; Snurr, R. Q.; Haag, W. O.; Kung, H. H. Monomolecular cracking of n-hexane on Y, MOR, and ZSM-5 zeolites. *Appl. Catal., A* **1999**, *179* (1), 71−86.
(44) Jones, A. J.; Carr, R. T.; Zones, S. I.; Iglesia, E. Acid strength and solvation in catalysis by MFI zeolites and effects of the identity, concentration and location of framework heteroatoms. *J. Catal.* **2014**, *312*, 58−68.
(45) Silaghi, M.-C.; Chizallet, C.; Sauer, J.; Raybaud, P. Dealumination mechanisms of zeolites and extra-framework aluminum confinement. *J. Catal.* **2016**, *339*, 242−255.
(46) Xue, N.; Vjunov, A.; Schallmoser, S.; Fulton, J. L.; Sanchez-Sanchez, M.; Hu, J. Z.; Mei, D.; Lercher, J. A. Hydrolysis of zeolite framework aluminum and its impact on acid catalyzed alkane reactions. *J. Catal.* **2018**, *365*, 359−366.
(47) Mezari, B.; Magusin, P. C.; Almutairi, S. M.; Pidko, E. A.; Hensen, E. J. Nature of Enhanced Brønsted Acidity Induced by Extraframework Aluminum in an Ultrastabilized Faujasite Zeolite: An In Situ NMR Study. *J. Phys. Chem. C* **2021**, *125*, 9050.
(48) Yi, X.; Peng, Y.-K.; Chen, W.; Liu, Z.; Zheng, A. Surface Fingerprinting of Faceted Metal Oxides and Porous Zeolite Catalysts by Probe-Assisted Solid-State NMR Approaches. *Acc. Chem. Res.* **2021**, *54*, 2421.
(49) van Bokhoven, J. A.; van der Eerden, A. M. J.; Koningsberger, D. C. Three-Coordinate Aluminum in Zeolites Observed with In situ X-ray Absorption Near-Edge Spectroscopy at the Al K-Edge: Flexibility of Aluminum Coordinations in Zeolites. *J. Am. Chem. Soc.* **2003**, *125* (24), 7435−7442.
(50) Chen, K.; Gan, Z.; Horstmeier, S.; White, J. L. Distribution of Aluminum Species in Zeolite Catalysts: 27Al NMR of Framework, Partially-Coordinated Framework, and Non-Framework Moieties. *J. Am. Chem. Soc.* **2021**, *143*, 6669.
(51) Mota, C. J. A.; Bhering, D. L.; Rosenbach, N., Jr. A DFT Study of the Acidity of Ultrastable Y Zeolite: Where Is the Brønsted/Lewis Acid Synergism? *Angew. Chem., Int. Ed.* **2004**, *43* (23), 3050−3053.
(52) Liu, C.; Li, G.; Hensen, E. J. M.; Pidko, E. A. Nature and Catalytic Role of Extraframework Aluminum in Faujasite Zeolite: A Theoretical Perspective. *ACS Catal.* **2015**, *5* (11), 7024−7033.
(53) Lukyanov, D. B.; Shtral, V. I.; Khadzhiev, S. N. A kinetic model for the hexane cracking reaction over H-ZSM-5. *J. Catal.* **1994**, *146* (1), 87−92.
(54) Konno, H.; Okamura, T.; Kawahara, T.; Nakasaka, Y.; Tago, T.; Masuda, T. Kinetics of n-hexane cracking over ZSM-5 zeolites - Effect of crystal size on effectiveness factor and catalyst lifetime. *Chem. Eng. J.* **2012**, *207*−*208*, 490−496.
(55) Gounder, R.; Iglesia, E. Catalytic Consequences of Spatial Constraints and Acid Site Location for Monomolecular Alkane Activation on Zeolites. *J. Am. Chem. Soc.* **2009**, *131* (5), 1958−1971.
(56) Wan, S.; Waters, C.; Stevens, A.; Gumidyala, A.; Jentoft, R.; Lobban, L.; Resasco, D.; Mallinson, R.; Crossley, S. Decoupling HZSM-5 Catalyst Activity from Deactivation during Upgrading of Pyrolysis Oil Vapors. *ChemSusChem* **2015**, *8* (3), 552−559.
(57) Abdelrahman, O. A.; Vinter, K. P.; Ren, L.; Xu, D.; Gorte, R. J.; Tsapatsis, M.; Dauenhauer, P. J. Simple quantification of zeolite acid site density by reactive gas chromatography. *Catal. Sci. Technol.* **2017**, *7* (17), 3831−3841.

https://doi.org/10.1021/acscatal.1c01138
ACS Catal. 2021, 11, 6982−6994